

Article

An Experimental Study on Seismic Performance Evaluation of Multi-Ply Bellows Type Expansion Joint for Piping Systems

Bub-Gyu Jeon ¹, Sung-Wan Kim ^{1,*}, Da-Woon Yun ¹, Bu-Seog Ju ^{2,*} and Ho-Young Son ²¹ Seismic Research and Test Center, Pusan National University, Yangsan 50612, Korea² Department of Civil Engineering, Kyung Hee University, Yongin 17104, Korea

* Correspondence: swkim09@pusan.ac.kr (S.-W.K.); bju2@khu.ac.kr (B.-S.J.)

Abstract: Piping systems are a representative social infrastructure to provide oil, gas, and water. Damage to piping systems may cause serious consequences, such as fire, water outage, and environmental pollution. Therefore, piping systems need to be protected from natural disasters, such as earthquakes. Earthquakes may cause deformation that exceeds piping design criteria. For example, large relative displacements and liquefaction of the ground resulting in loss of strength and ground subsidence, and the side-sway of primary structures subjected to a strong ground motion may cause critical damage to piping systems. Therefore, expansion joints to maintain flexibility can be applied to locations where excessive deformation is expected to improve the seismic performance of piping systems. Metal bellows, a type of expansion joints, are flexible, so they are highly durable against deformation and fatigue loads. This indicates that metal bellows can be used as seismic separation joints for piping. In this study, experimental research was conducted to analyze the seismic performance of multi-ply bellows type expansion joints, a type of metal bellows. Monotonic loading tests and cyclic loading tests were conducted on 2-ply bellows and 3-ply bellows, and the results were compared. In the cyclic loading tests, multi-step increasing amplitude cyclic loading, which used the displacement history amplified in stages, and constant amplitude cycling loading with various magnitudes were considered. The test results showed no significant difference in bending performance for monotonic loading between the two types of multi-ply bellows. The 3-ply bellows, however, showed higher performance for low-cycle fatigue than 2-ply bellows.

Keywords: expansion joint; seismic performance; bellows; piping system

Citation: Jeon, B.-G.; Kim, S.-W.; Yun, D.-W.; Ju, B.-S.; Son, H.-Y. An Experimental Study on Seismic Performance Evaluation of Multi-Ply Bellows Type Expansion Joint for Piping Systems. *Sustainability* **2022**, *14*, 14777. <https://doi.org/10.3390/su142214777>

Academic Editor: Humberto Varum

Received: 28 September 2022

Accepted: 7 November 2022

Published: 9 November 2022

Publisher's Note: MDPI stays neutral with regard to jurisdictional claims in published maps and institutional affiliations.



Copyright: © 2022 by the authors. Licensee MDPI, Basel, Switzerland. This article is an open access article distributed under the terms and conditions of the Creative Commons Attribution (CC BY) license (<https://creativecommons.org/licenses/by/4.0/>).

1. Introduction

The frequency of earthquakes worldwide is increasing each year, and the scale of expected seismic damage is also increasing due to the urban population and the expanding size of facilities due to industrial development [1–3]. Piping has been widely used in most industries as the major equipment for providing gas or liquid. Thus, the integrity of a piping system is very important for maintaining its original function and for the safety of facilities. Strong external forces can cause seismic-induced damage or malfunction to the piping system. In particular, leakage can cause serious secondary damage, such as explosion or liquefaction. Therefore, pipes must have sufficient seismic performance to prevent damage against earthquakes that have been assumed during the design process.

In general, piping is buried underground or installed using the support of structures. Buried piping systems can be damaged by permanent ground deformation (PGD), such as soil liquefaction, fault, and ground subsidence [4,5]. Seismic damage to buried piping is mainly found at joints [6]. The piping installed in structures is damaged by the deformation and story drift of the structures as well as the relative displacement between the structures [7]. Damage occurs due to the concentration of nonlinear behavior on supports, joints, and fittings (elbow, tee) [8]. The main cause of seismic damage to piping is the relative displacement that exceeds the allowable displacement, with the joints and fittings

as a critical damaged location. Therefore, experimental research to analyze the seismic behavior of piping with joints and fittings, as well as assess its seismic performance, has attracted significant attention of many researchers.

To evaluate the seismic performance of buried piping, tensile, compressive, and bending tests have been conducted on piping with various specifications. In particular, various studies have been conducted recently to analyze the seismic behavior of piping systems considering buried conditions [9–13]. Research on piping that is installed in structures has also been conducted in various industrial fields. Experimental studies were conducted to analyze the nonlinear behavior of piping elements under internal pressure and seismic loading conditions [14,15], and the low-cycle fatigue and limit state of the piping system was defined in these studies [16–21]. A program was also performed to analyze the gap between plastic collapse corresponding to the design standard consideration and leakage related to the actual failure observed through experimental tests and to simulate the extreme nonlinear behavior of piping [22]. In recent years, studies have been actively conducted to analyze the seismic behavior of non-welded joints or supports in piping [23–26]. Through-wall cracks were defined as failure criteria, and seismic fragility was analyzed in piping systems [27,28].

Seismic separation joints in piping are installed at locations where earthquake-induced deformation is concentrated to protect the piping [29]. Bellows-type expansion joints are devices that absorb the expansion and deformation of pipes caused by the temperature difference and to prevent the damage caused by mechanical vibration. They are highly adaptable to relatively large deformations due to their flexibility and low stiffness. As a result, well-designed bellows-type expansion joints can be applied to improve the seismic performance of piping [30]. However, very few studies of the current state of bellows piping joints have evaluated the structural performance or seismic performance of the expansion joints based on experimental data. Thus, an experimental study that considers the characteristics of seismic loads is required. In this study, bending tests were conducted to evaluate the seismic performance of bellows-type expansion joints. Monotonic loading tests and cyclic loading tests were conducted on two types of multi-ply metal bellows with multi-layered structures. The cyclic loading tests were divided into multi-step loading conditions with (1) increasing amplitude cyclic loading tests, which applied the displacement history amplified in stages, and (2) constant amplitude cyclic loading tests, which considered a constant amplitude in various magnitudes. Finally, the test results of the two types of multi-ply metal bellows were compared, and their seismic performance and low-cycle fatigue performance were predicted.

2. Test Specimen

Bellows forming methods can be mainly classified into mechanical and hydraulic forming methods. In mechanical forming methods, a tube is placed on a forming machine, and each convolution is formed using the pressure applied by the forming roll while rotating. In hydraulic forming methods, a tube is placed on a hydraulic press or forming machine, and a circular mold is arranged on the outside of the tube. The inside of the tube is then filled with water, and a product is formed by applying pressure until yielding in the circumferential direction occurs. Hydroforming is a representative hydraulic forming method. Bellows may exhibit the yielding of materials during the forming process, and the hardness may change. The bellows formed using the hydroforming method, however, can minimize the increase in hardness by work hardening compared to mechanical forming [31]. Therefore, in this study, tests were conducted on the multi-ply metal bellows type expansion joints fabricated using the hydroforming method.

Figure 1 shows multi-ply metal bellows. In general, bellows are formed using a single-layer steel sheet. To improve the low-cycle fatigue performance of bellows, 2-ply or 3-ply structures can be considered, as shown in Figure 1. In this study, 2-ply metal bellows type expansion joints were defined as 2-ply bellows, and in a similar manner, 3-ply metal bellows type expansion joints were defined as 3-ply bellows. The bellows of the test

specimens were fabricated by overlapping STS 316L stainless steel sheets with a thickness of 0.3 mm. The thickness of the 2-ply bellows was 0.6 mm, and that of the 3-ply bellows was 0.9 mm.

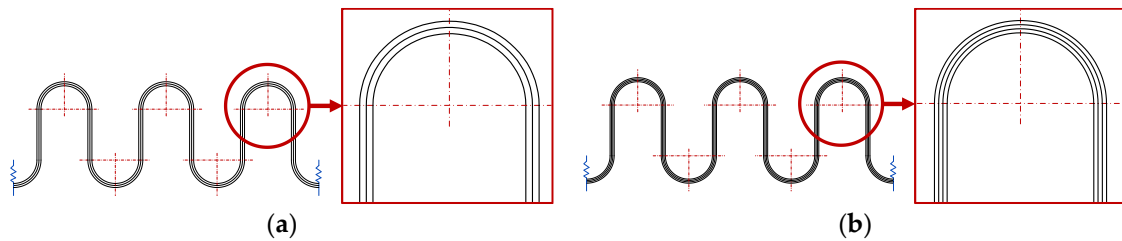


Figure 1. Multi-ply bellows: (a) 2-ply bellows, (b) 3-ply bellows.

In this study, it was assumed that multi-ply metal bellows type expansion joints were applied to gas systems piping. Carbon steel pipes for fuel gas piping have various standards [32]. In general, the standard piping of 100 mm or less is used for the supply to residential areas. For this study, test specimens were prepared considering piping with an outer diameter of 89.1 mm. Figure 2a,b shows the schematic designs and a photograph of a test specimen. The U-shaped bellows located in the center of the test specimen had six convolutions, a pitch of 15 mm, a height of 15 mm, and a length of 110 mm. The bellows were connected to 50 mm-long SS275 carbon steel pipes [33] by welding, and the ends of the straight pipes were finished with flanges. Table 1 shows the material properties of STS 316L provided by the manufacturer.

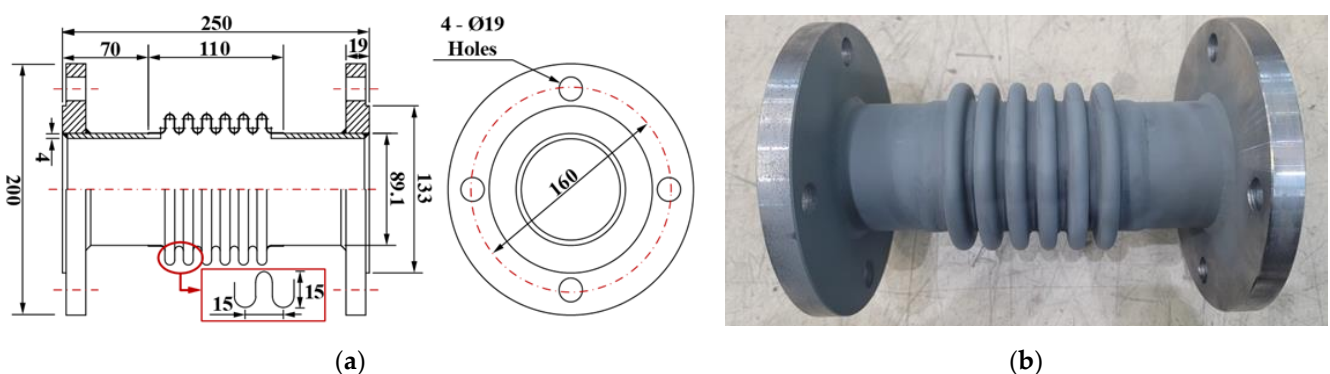


Figure 2. Test specimen: (a) Schematic design of test specimen, (b) manufacturing product of test specimen.

Table 1. Material properties.

	Yield Strength (N/mm ²)	Tensile Strength (N/mm ²)	Elongation (%)
STS 316L	257	563	52.7

3. Test Setup and Method

Figure 3a shows the test setup, and Figure 3b is a photograph of the setup. As shown in Figure 3a, one end of the test specimen was connected to the jig fixed at the bottom of the universal testing machine (UTM), while the other end was connected to the jig fixed at the actuator using a pin. This design describes the bending deformation caused by the external force applied in the direction perpendicular to the axis to be concentrated on the bellows. In addition, the degree of freedom in directions other than the loading direction was constrained using the LM guide. The inside of the specimen was filled with water, and a pressure of 0.4 MPa [34] was applied using a regulator and a pump before the experiment. The pressure was maintained until the end of the experiment. In this study, pipe damage

was defined as leakage, and the experiment was performed until leakage occurred. This experiment was carried out using 1000 kN UTM in the Seismic Research and Test Center at Pusan National University.

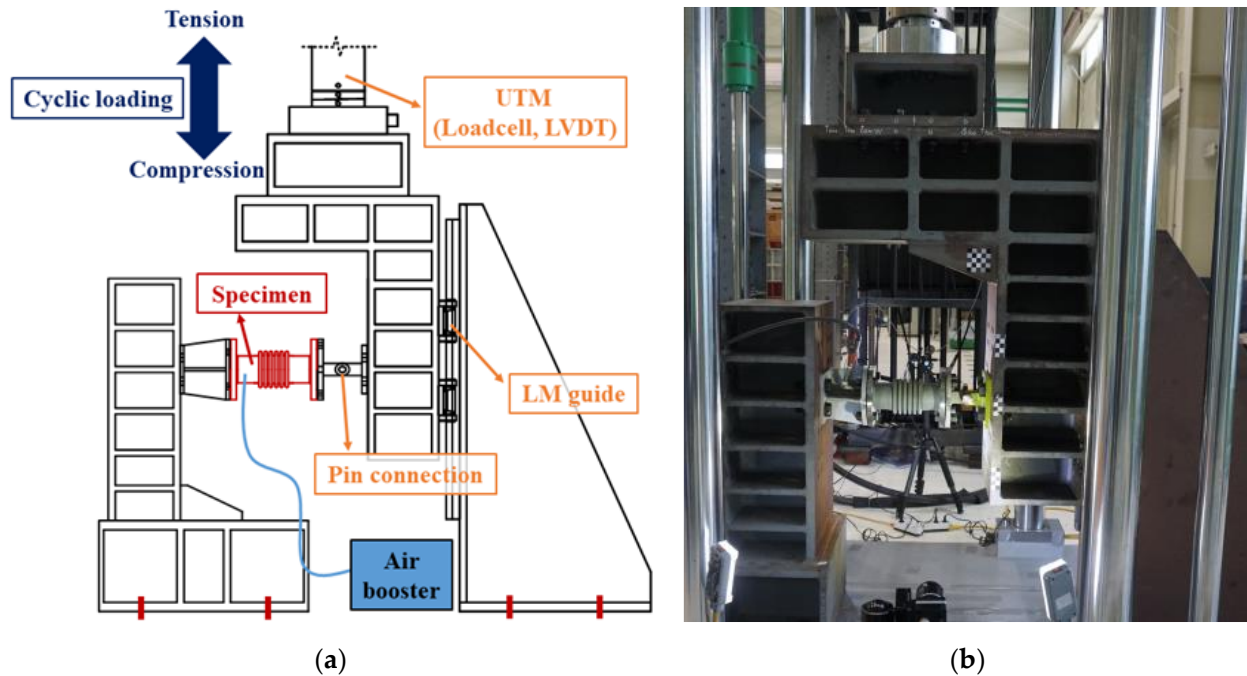


Figure 3. Test configuration: (a) Test set up, (b) test photo.

Figure 4 shows the test procedure. First, the monotonic loading test is conducted. Then the multi-step increasing amplitude cyclic loading test is conducted by setting 25% of the minimum leakage displacement of the monotonic loading test as the initial amplitude. Based on the magnitude of the cycle that preceded the cycle where leakage occurred in the multi-step increasing amplitude cyclic loading test (minimum displacement of the two test results), the constant amplitude cyclic loading test is carried out. As shown in Figure 4, the objective of the monotonic loading test and multi-step increasing amplitude cyclic loading test are focused on the evaluation of the seismic performance of the bellows piping system, whereas the constant amplitude cyclic loading test is a low-cycle fatigue test.

The monotonic loading test was conducted until leakage occurred in the tension direction in Figure 3. The multi-step increasing amplitude cyclic loading test used the two-step displacement cyclic loading history, as shown in Figure 5, and this was continued until leakage occurred. The cyclic loading history was prepared by referring to ANSI/FM Approvals 1950 [35] and KS B 1528 [36]. ANSI/FM Approvals 1950, a test method to evaluate the seismic performance of a seismic sway brace in piping, proposes a cyclic loading test by a test frequency of 0.1 Hz or less. In this test method, the cyclic loading process is performed 15 times for the initial amplitude, and the magnitude of the amplitude is gradually increased. Here, the initial amplitude must be less than 50% of the expected damage load, and the 15 cycles mean one seismic event [37]. KS B 1528 suggests a test method for pipe joints by referring to ANSI/FM Approvals 1950. The cyclic loading history of this test method is similar to that of ANSI/FM Approvals 1950, but the amplitude is proposed as an angle to consider the deformation of piping by the story drift of the structure. For the initial amplitude, the deformation angle of the pipe joint by the story drift of the structure was considered. In the case of FEMA 461 [38], the cyclic loading history gradually increased by displacement control that takes into account the story drift of the structure. Since seismic separation joints are applied to locations where relative displacement may occur, it was determined that tests must be conducted with displacement control. Therefore, in this study, the cyclic loading history shown in Figure 5 was used.

After applying cyclic loads 15 times for x , which is the initial amplitude and as shown in Equation (1), the amplitude is increased until leakage occurs according to Equation (2). Here, Δl is the loading amplitude and N is the number of cycles.

$$\Delta l = x \quad \text{for } N \leq 15 \text{ cycles} \tag{1}$$

$$\Delta l = x \times \left(\frac{15}{14}\right)^{\frac{(N-15)}{2}} \quad \text{for } N > 15 \text{ cycles} \tag{2}$$

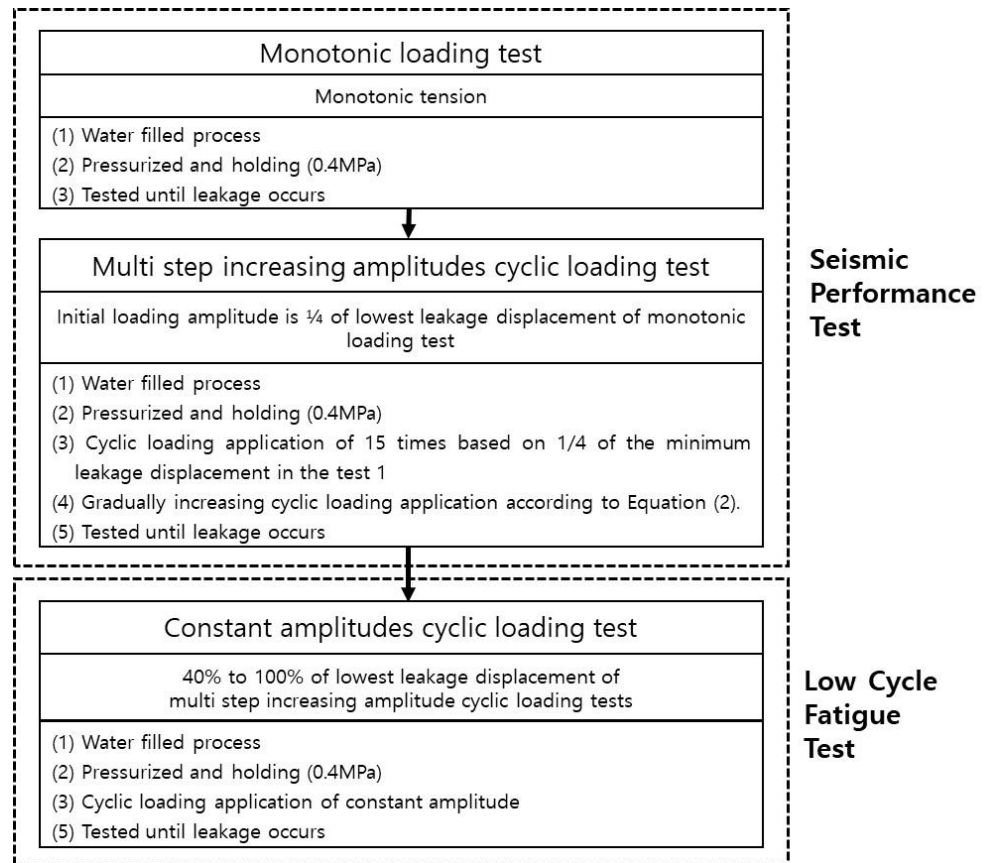


Figure 4. Experimental test workflow.

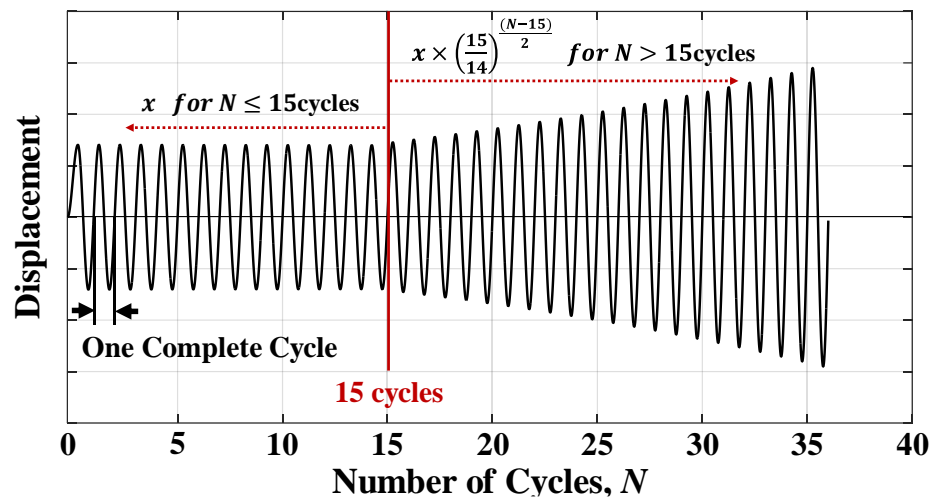


Figure 5. Displacement history for multi-step increasing amplitude cyclic loading test.

The constant amplitude cyclic loading test was conducted to estimate low-cycle fatigue life. For the loading amplitude, the amplitude of the cycle before the minimum leakage displacement of the multi-step increasing amplitude cyclic loading test was defined as 100%, and 40% to 100% was applied at 10% intervals. Both the monotonic loading test and multi-step increasing amplitude cyclic loading test were performed twice, and the constant amplitude cyclic loading test was conducted once for each input amplitude. All the tests were conducted at a rate of 1 mm/s or less.

The deformation angle is a representative performance required for seismic separation joints [29,36,39]. In this study, the deformation angle was calculated using the center of the fixed flange and the center of the pin connection, as shown in Figure 6, and l is the length of the test specimen and θ is the deformation angle.

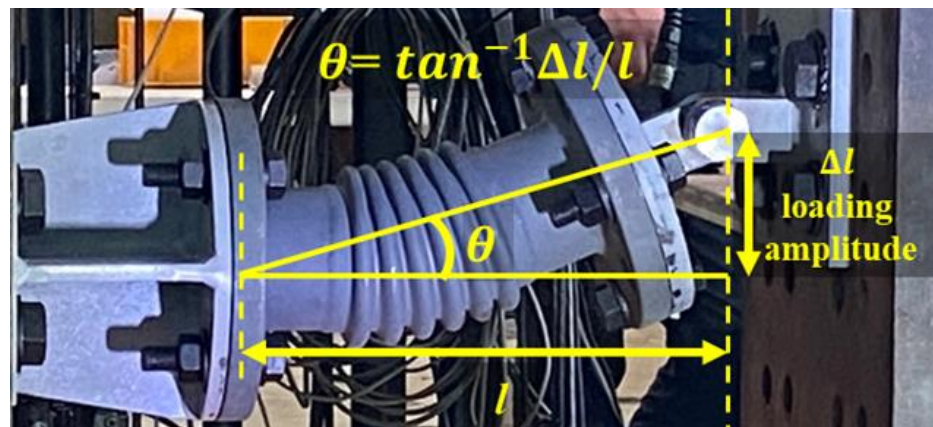


Figure 6. Estimation of deformation angle.

4. Experiment Results and Analysis

Tables 2 and 3 show the bending test results of 2-ply bellows and 3-ply bellows, respectively. When expressed to one decimal point for both 2-ply bellows and 3-ply bellows, 25% of the minimum leakage displacement in the monotonic loading test was 59.0 mm. Therefore, 59.0 mm was used as the initial amplitude of the multi-step increasing amplitude cyclic loading tests. In the monotonic loading test of 2-ply bellows, leakage displacements were 257.8 and 237.1 mm with a difference of 8.4%, while the leakage angles were 39.8° and 37.5° with a difference of 6.0%. In the multi-step increasing amplitude cyclic loading test, leakage displacement and leakage angle were found to be 113.6 mm and 20.2° in both tests. Therefore, the difference of the multi-step increasing amplitude cyclic loading test is 0.0%, as shown in Table 4. In the monotonic loading test of 3-ply bellows, the leakage displacements were 237.0 and 248.7 mm with a difference of 4.8%, while the leakage angles were 37.5° and 38.8° with a difference of 3.4%. In the multi-step increasing amplitude cyclic loading test, leakage displacements were 126.0 and 130.5 mm with a difference of 3.5%, while the leakage angles were 22.2° and 22.9°, with a difference of 3.1%. Table 4 shows the difference in leakage points between the 2-ply bellows and 3-ply bellows in the same test. The difference was calculated using Equation (3) with E_1 and E_2 as experimental values.

$$\text{Difference (\%)} = \frac{|E_1 - E_2|}{\frac{1}{2}(E_1 + E_2)} \times 100 \quad (3)$$

Table 2. Test results of 2-ply bellows.

Test Method	No.	Leakage Point			N_f	Remarks
		Displacement (mm)	Angle (Degree)	Location		
Monotonic	2P-M1	257.8	39.8	Pipe-bellows welding	-	Lowest leakage displacement: 237.1 mm
	2P-M2	237.1	37.5		-	
Multi-step increasing amplitude cyclic	2P-MC1	113.6	20.2	Convolutions of bellows	34	Initial amplitude: 59 mm
	2P-MC2	113.6	20.2		34	
Constant amplitude cyclic	2P-C1	44.0	8.1	Convolutions of bellows	592	Amp. 40%
	2P-C2	55.0	10.1		74	Amp. 50%
	2P-C3	66.0	12.1		43	Amp. 60%
	2P-C4	77.0	14.0		22	Amp. 70%
	2P-C5	88.0	15.9		17	Amp. 80%
	2P-C6	99.0	17.8		13	Amp. 90%
	2P-C7	110.0	19.6		6	Amp. 100%: Amplitude of cycle before minimum leakage displacement at multi-step increasing amplitude cyclic test

Table 3. Test results of 3-ply bellows.

Test Method	No.	Leakage Point			N_f	Remarks
		Displacement (mm)	Angle (Degree)	Location		
Monotonic	3P-M1	237.0	37.5	Pipe-bellows welding	-	Lowest leakage displacement: 237 mm
	3P-M2	248.7	38.8		-	
Multi-step increasing amplitude cyclic	3P-MC1	126.0	22.2	Convolutions of bellows	37	Initial amplitude: 59 mm
	3P-MC2	130.5	22.9		38	
Constant amplitude cyclic	3P-C1	48.8	9.0	Convolutions of bellows	1949	Amp. 40%
	3P-C2	61.0	11.2		406	Amp. 50%
	3P-C3	73.2	13.3		153	Amp. 60%
	3P-C4	85.4	15.4		46	Amp. 70%
	3P-C5	97.6	17.5		10	Amp. 80%
	3P-C6	109.8	19.6		7	Amp. 90%
	3P-C7	122.0	21.5		4	Amp. 100%: Amplitude of cycle before minimum leakage displacement at multi-step increasing amplitude cyclic test

Table 4. Difference in leakage points.

	Difference in Leakage Point (%)			
	2-Ply Bellows		3-Ply Bellows	
	Displacement	Angle	Displacement	Angle
Monotonic	8.4	6.0	4.8	3.4
Multi-step increasing amplitude cyclic	0.0	0.0	3.5	3.1

Tables 2 and 3, the number of cycles to failure (N_f) increases as the magnitude of the input amplitude increases. For 2-ply bellows, N_f is 74 cycles or less when the magnitude is 50% or higher and 592 cycles when it is 40%. In the case of 3-ply bellows, N_f is 406 cycles or less when the magnitude is 50% or higher and 1949 cycles when it is 40%.

Table 5 compares the minimum leakage points of the monotonic loading test and the multi-step increasing amplitude cyclic loading test. The ratio between the leakage displacement of the multi-step increasing amplitude cyclic loading test and that of the monotonic loading test is 0.48 for 2-ply and 0.53 for 3-ply. These become 0.5 when rounded to the first decimal place. The leakage angle ratio is 0.54 for 2-ply and 0.59 for 3-ply, and these become 0.6 or less when rounded to the first decimal place.

Table 5. Minimum leakage points comparison of monotonic and multi-step increasing cyclic loading tests.

Specimen Type	Leakage Displacement		Leakage Angle		Ratio (MC/M)	
	Monotonic [M]	Multi-Step Increasing Cyclic Loading [MC]	Monotonic [M]	Multi-Step Increasing Cyclic Loading [MC]	Leakage Displacement	Leakage Angle
2-ply	237.1 mm	113.6 mm	37.5°	20.2°	0.48	0.54
3-ply	237.0 mm	126.0 mm	37.5°	22.2°	0.53	0.59
Difference	0.0%	10.4%	0.0%	9.4%	-	-

The difference in the minimum leakage point of the monotonic loading test between 2-ply bellows and 3-ply bellows is insignificant when expressed to the first decimal place. For the minimum leakage points of the multi-step increasing amplitude cyclic loading test, however, the leakage displacement is 10.4% higher, and the leakage angle is 9.4% higher for 3-ply bellows compared to 2-ply bellows.

Figures 7–9 show the leakage in each test, with a yellow circle marking the leakage location. In the monotonic loading test, leakage caused by cracking in the bellows-pipe weld was observed. Figures 8 and 9 show the leakage locations of the multi-step increasing amplitude cyclic loading test and constant amplitude cyclic loading test, respectively. The cyclic loading test results showed that leakage occurred due to the through-wall cracks generated in the loading direction in the convolution of the bellows. Water spray can be seen in the yellow circles of Figures 8 and 9. Leakage locations vary between the monotonic loading test and the cyclic loading test. In the same test, however, the leakage locations of 2-ply bellows and 3-ply bellows are similar.



Figure 7. Leakage of monotonic bending tests: (a) 2-ply bellows, (b) 3-ply bellows.



Figure 8. Leakage of multi-step increasing amplitude cyclic loading tests: (a) 2-ply bellows, (b) 3-ply bellows.



Figure 9. Leakage of constant amplitude cyclic bending tests: (a) 2-ply bellows specimen, (b) 3-ply bellows specimen.

Figure 10a shows the load-displacement correlation measured from the monotonic loading test of 2-ply bellows. The load and displacement are the responses measured from the load cell and the displacement meter in the actuator of UTM. As shown in Table 4, the difference in leakage displacement is 8.4%. The maximum loads, however, are 38.1 and 31.5 kN, respectively, with a difference of 19.0%. Figure 10b shows the load-displacement correlation of 3-ply bellows. The difference in leakage displacement between the two test specimens is not significant (4.8%). The maximum loads, however, are 39.8 and 56.8 kN, respectively, with a difference of 35.2%. From Figure 10, it can be seen that the load at leakage is 8.3 kN (approximately 1.3 times) to 25.3 kN (1.8 times) higher for 3-ply bellows compared to 2-ply bellows. As shown in Figures 7 and 10, it was estimated that the damage of the test specimen due to monotonic loading tests could not occur due to fatigue, but damage to the welded part occurred due to exceeding the limit displacement. Therefore, it is estimated that the damage displacement is similar, but the load could be higher with 3-ply bellows specimens.

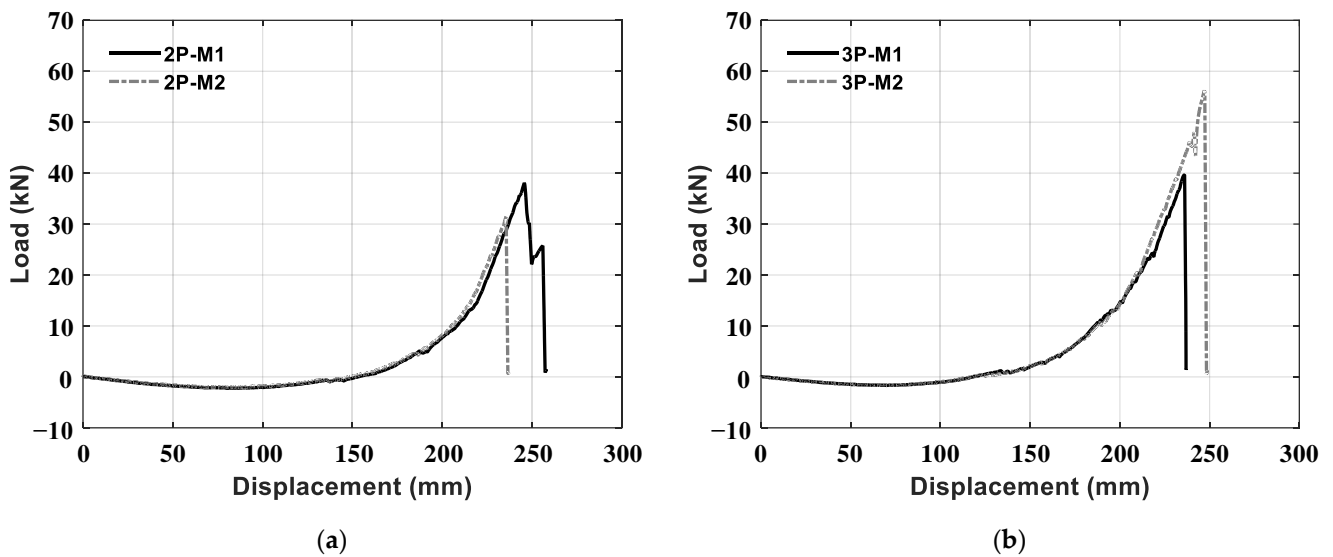


Figure 10. Load-displacement relationship of monotonic bending tests: (a) 2-ply bellows, (b) 3-ply bellows.

Figure 11 shows the load-displacement hysteresis loops of the multi-step increasing amplitude cyclic loading test. For the 2-ply bellows shown in Figure 11a, the load tends to decrease in the initial 15-cycle section. This phenomenon, however, is not significant for 3-ply bellows. Figures 12 and 13 show the load-displacement hysteresis loops of 2-ply bellows and 3-ply bellows in the constant amplitude cyclic loading test, respectively. The load tends to decrease as the number of cycles increases. In Figure 12, the load tends to decrease in all tests for 2-ply bellows. In the case of 3-ply bellows, however, the load tends to significantly decrease as the number of cycles increases at an input amplitude of 61 mm (50%) or less, as shown in Figure 13a.

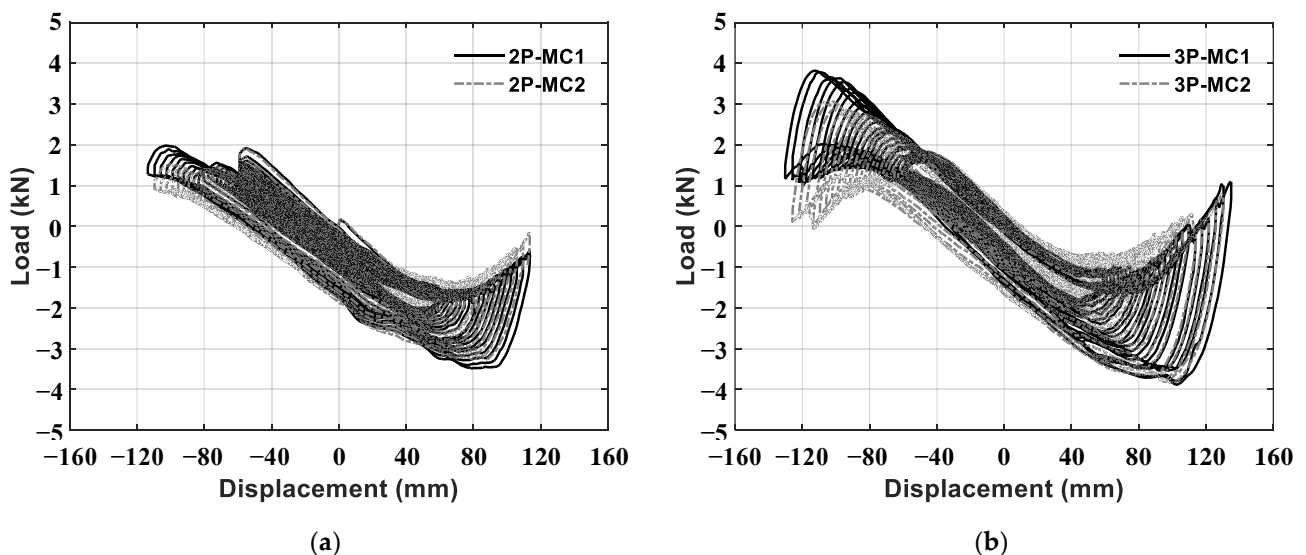


Figure 11. Load-displacement relationship of multi-step increasing amplitude cyclic loading tests: (a) 2-ply bellows, (b) 3-ply bellows.

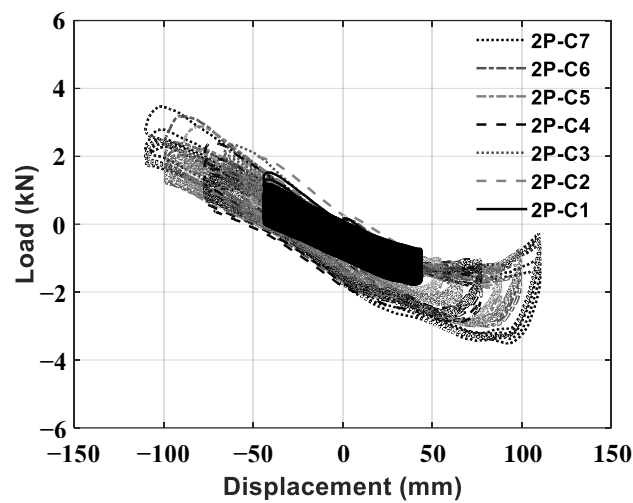


Figure 12. Load-displacement relationship of constant amplitude cyclic loading tests of 2-ply bellows.

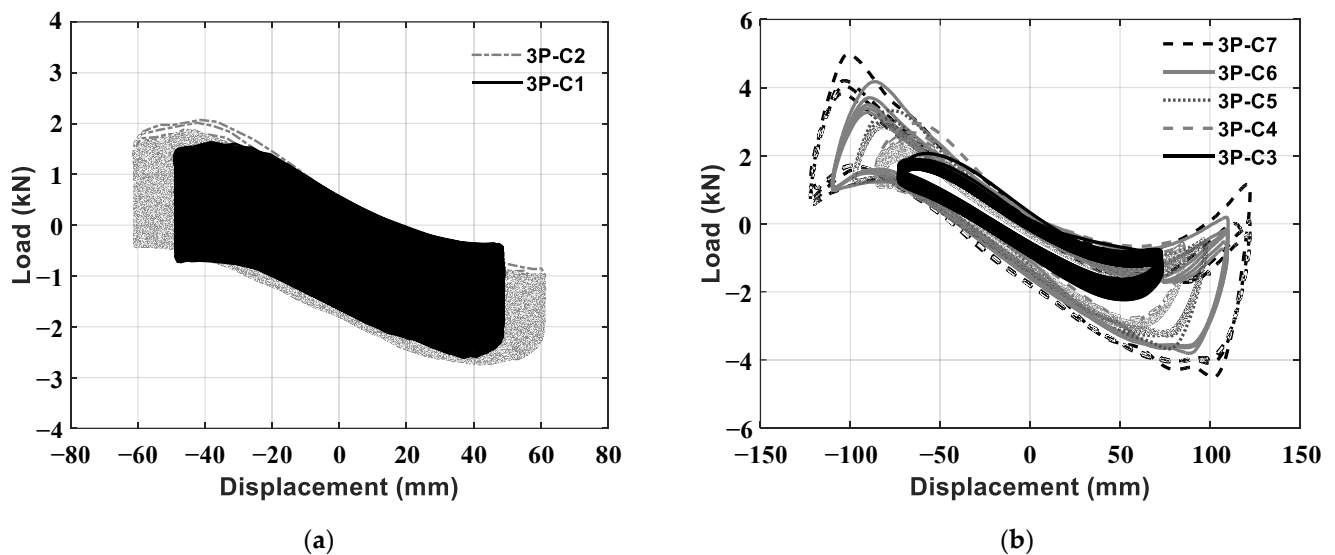


Figure 13. Load-displacement relationship of constant amplitude cyclic loading tests of 3-ply bellows: (a) Load-displacement relationship of amplitude 50% or less, (b) load-displacement relationship of amplitude 50% or more.

Next, an additional study associated with the damage criteria of bellows piping system was proposed in this study. Fatigue failure is a phenomenon in which an object subjected to repeated small forces develops fractures due to cracking. Among the fatigue phenomena, fatigue failure with a low repetition frequency is defined as low-cycle fatigue. In Tables 2 and 3, N_f significantly increases when the input amplitude is 40% (44 mm) for 2-ply bellows. For 3-ply bellows, N_f significantly increases when the input amplitude is 40% (48.8 mm). Therefore, in this study, the low-cycle fatigue curve was estimated for cases where N_f was smaller than 500 cycles.

The low-cycle fatigue life of the seismic vulnerability components of piping could be estimated using the relationship between the loading amplitude and N_f by the cyclic loading test [34,35]. Figure 14 shows the leakage displacement- N_f relationship and the low-cycle fatigue curve of multi-ply bellows-type expansion joints. Here, the low-cycle fatigue of 2-ply bellows can be represented by Equation (4) and that of 3-ply bellows by Equation (5). Figure 15 shows the leakage angle- N_f relationship and the low-cycle fatigue curve. Equations (6) and (7) present the low-cycle fatigue curves of 2-ply bellows and 3-ply bellows by the leakage angle- N_f relationship, respectively. From Figure 15, it can be

seen that 3-ply bellows have higher low-cycle fatigue performance than 2-ply bellows. For Equations (4)–(7), the coefficient of determination (R^2) is 0.97 or higher, indicating high reliability. Here, δ refers to the leakage displacement, and θ is the leakage angle.

$$\delta_{2\text{ply}} = 192.18 N_f^{-0.286} \quad R^2 = 0.9723 \quad (4)$$

$$\delta_{3\text{ply}} = 143.14 N_f^{-0.139} \quad R^2 = 0.9807 \quad (5)$$

$$\theta_{2\text{ply}} = 33.497 N_f^{-0.273} \quad R^2 = 0.9704 \quad (6)$$

$$\theta_{3\text{ply}} = 25.107 N_f^{-0.131} \quad R^2 = 0.9820 \quad (7)$$

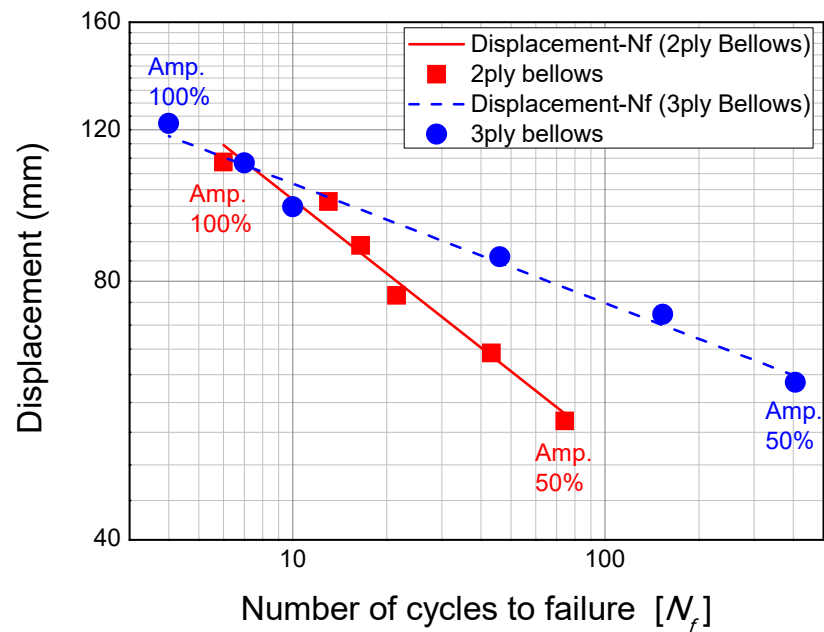


Figure 14. Low-cycle fatigue curve of multi-ply bellows based on leakage displacement.

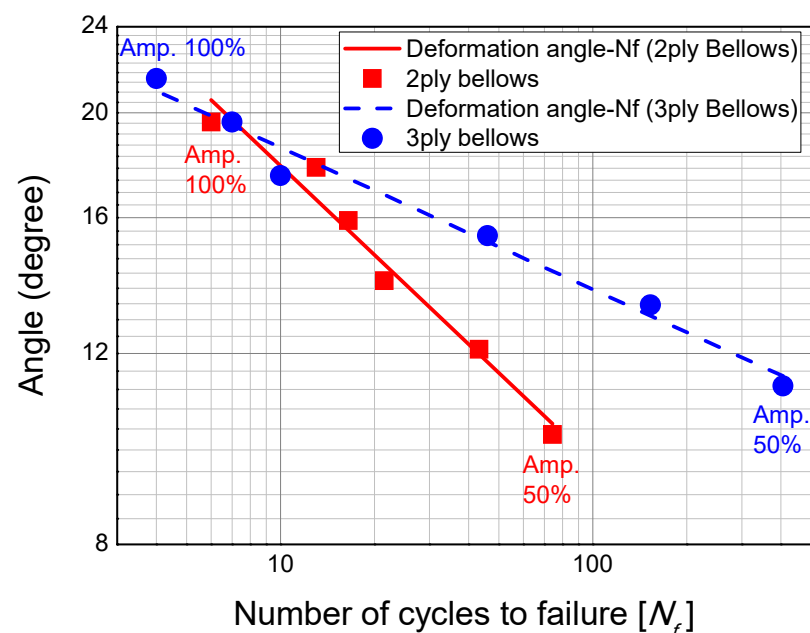


Figure 15. Low-cycle fatigue curve of multi-ply bellows based on leakage angle.

Table 6 compares the leakage points of the monotonic test with those of the constant amplitude cyclic loading test with an input amplitude of 50%. The minimum leakage displacement ratio between the constant amplitude cyclic loading test and the monotonic test is 0.23 for 2-ply and 0.26 for 3-ply, respectively. These changed to 0.2 and 0.3 when rounded to the first decimal place. In other words, they are smaller than 0.3. The minimum leakage angle ratio is 0.27 and 0.30 for 2-ply and 3-ply, respectively. These become 0.3 when rounded to the first decimal place. Therefore, for the multi-ply bellows used in this study, the leakage point ratio between the constant amplitude cyclic loading test with an input amplitude of 50% and the monotonic test is 0.3 or less.

Table 6. Comparison of leakage points for bending test.

Specimen Type		2-Ply Bellows		3-Ply Bellows	
	Unit	Minimum Leakage Displacement (mm)	Minimum Leakage Angle (Degree)	Minimum Leakage Displacement (mm)	Minimum Leakage Angle (Degree)
Leakage point	Monotonic [M]	237.1	37.5	237	37.5
	Amplitude 50% of constant amplitude cyclic loading [Amp. 50%]	55.0	10.1	61	11.2
Ratio of failure	Amp. 50%/M	0.23	0.27	0.26	0.30

5. Conclusions

In this study, the seismic performance of multi-ply metal bellows type expansion joints was evaluated through monotonic loading tests and multi-step increasing amplitude cyclic loading tests. The influence of low-cycle fatigue was also analyzed through constant amplitude cyclic loading tests.

The leakage point of the monotonic loading tests was observed at the location of the weld area between the bellows and the pipe. The leakage location in the increasing amplitude and constant amplitude cyclic loading tests, however, is the convolution of the bellows, indicating that damage locations differ between monotonic loading and cyclic loading.

There is no significant difference in the minimum leakage points of the monotonic loading tests between 2-ply bellows and 3-ply bellows. The leakage points of the multi-step increasing amplitude cyclic loading tests, however, are more than 9% higher for 3-ply bellows compared to 2-ply bellows. This indicates that the low-cycle fatigue performance becomes higher as the number of layers in bellows increases. In this study, it was assumed that low-cycle fatigue occurred when the number of cycles to failure (N_f) exceeded 500 cycles. Therefore, a low-cycle fatigue curve was designed for an input amplitude of 50% or higher in the constant amplitude cyclic loading test. Consequently, it was found that 3-ply bellows have higher low-cycle fatigue performance than 2-ply bellows. Therefore, it is estimated that the seismic performance of 3-ply bellows could be better than 2-ply bellows.

For both 2-ply bellows and 3-ply bellows, the minimum leakage displacement of the multi-step increasing amplitude cyclic loading tests is less than 53% of that of monotonic loading tests. Low-cycle fatigue occurs at less than 26% of the minimum leakage displacement of the monotonic loading tests. In addition, the minimum leakage angle of the multi-step increasing amplitude cyclic loading tests is less than 60% of that of monotonic loading tests. The magnitude of the deformation angle at which low-cycle fatigue is observed is also smaller than 30% of the minimum leakage angle of the monotonic loading tests.

In the multi-step increasing amplitude cyclic loading tests conducted in this study, 15 cycles by the initial amplitude indicate one seismic event. Therefore, the cumulative plastic deformation attributed to low-cycle fatigue must be minimized at this stage. In

addition, when seismic performance is evaluated using the cyclic loading history used in this study, the appropriate magnitude of the initial amplitude of the multi-step increasing amplitude cyclic loading test is less than 25% of the leakage displacement of the monotonic loading test or less than 30% of the leakage angle.

The results of this study can be used as data for the seismic design of bellows-type expansion joints. They can also be used as basic data to consider relative seismic displacement when performance verification and experimental research are conducted for the application of bellows-type expansion joints.

Author Contributions: Conceptualization, B.-G.J. and S.-W.K.; methodology, B.-S.J.; software, D.-W.Y.; validation, H.-Y.S., B.-G.J. and S.-W.K.; formal analysis, B.-S.J.; investigation, H.-Y.S.; resources, B.-G.J.; data curation, D.-W.Y.; Writing—Original draft preparation, B.-G.J. and S.-W.K.; Writing—Review and Editing, B.-G.J. and B.-S.J. All authors have read and agreed to the published version of the manuscript.

Funding: This research was funded by the Korea Agency for Infrastructure Technology Advancement (KAIA) grant funded by the Ministry of Land, Infrastructure and Transport of Korean Government (No. 22CTAP-C164263-02).

Institutional Review Board Statement: Not applicable.

Informed Consent Statement: Not applicable.

Data Availability Statement: The data presented in this study are available on request from the corresponding author.

Acknowledgments: The authors gratefully acknowledge support by the research fund of the Korea Agency for Infrastructure Technology Advancement (KAIA) grant funded by the Ministry of Land, Infrastructure and Transport of Korean government (No. 22CTAP-C164263-02).

Conflicts of Interest: The authors declare no conflict of interest.

References

- Perrone, D.; Calvi, P.M.; Nascimbene, R.; Fischer, E.C.; Magliulo, G. Seismic performance of non-structural elements during the 2016 Central Italy earthquake. *Bull. Earthq. Eng.* **2019**, *17*, 5655–5677. [CrossRef]
- Belleri, A.; Brunesi, E.; Nascimbene, R.; Pagani, M. Seismic Performance of Precast Industrial Facilities Following Major Earthquakes in the Italian Territory. *J. Perform. Constr. Facil.* **2015**, *29*, 04014135. [CrossRef]
- Brunesi, E.; Nascimbene, R.; Pagani, M.; Beilic, D. Seismic Performance of Storage Steel Tanks during the May 2012 Emilia, Italy, Earthquakes. *J. Perform. Constr. Facil.* **2015**, *29*, 04014137. [CrossRef]
- Yasuda, S.; Kiku, H. Uplift of sewage manholes and pipes during the 2004 Niigataken-chuetsu earthquake. *Soils Found.* **2006**, *46*, 885–894. [CrossRef]
- Yasuda, S.; Harada, K.; Ishikawa, K.; Kanemaru, Y. Characteristics of liquefaction in Tokyo Bay area by the 2011 Great East Japan Earthquake. *Soils Found.* **2012**, *52*, 793–810. [CrossRef]
- Donald, B. Understanding the Seismic Vulnerability of Water Systems. 2013. Available online: <https://docplayer.net/7985651-ofWaterUnderstanding-the-seismic-vulnerability-of-water-systems.html> (accessed on 2 October 2013).
- American Society of Civil Engineers; Structural Engineering Institute (ASCE/SEI). *ASCE 7–16: Minimum Design Loads and Associated Criteria for Buildings and Other Structures*; ASCE: Reston, VA, USA, 2017.
- Kim, S.W.; Jeon, B.G.; Ahn, S.W.; Wi, S.W. Seismic behavior of riser pipes with pressure and groove joints using an in-plane cyclic loading test. *J. Build. Eng.* **2021**, *34*, 101911. [CrossRef]
- Edkins, D.J.; Orense, R.P.; Henry, R.S. Seismic simulation testing of PVC-U pipe and proposed design prediction tool for joint performance. *J. Pipeline Syst. Eng. Pract.* **2021**, *12*, 04021007. [CrossRef]
- Ihnotic, C.R.; Ramos, J.L.; Wham, B.P. *Seismic Evaluation of Hazard-Resistant Pipelines: PVC, PVCO, and iPVC Pipe with Coupling*; University of Colorado Boulder: Boulder, CO, USA, 2019.
- Wham, B.P.; O'Rourke, T.D.; Stewart, H.E.; Bond, T.K.; Pariya-Ekkasut, C. *Large-Scale Testing of JFE Steel Pipe Crossing Faults: Testing of SPF Wave Feature to Resist Fault Rupture*; Cornell University: Ithaca, NY, USA, 2016.
- Lv, Y.; Liu, C.F.; Huang, X.; Chen, Y.; Chouw, N. Experimental and finite-element studies of buried pipes connected by a bellow joint under cyclic shear loading. *J. Pipeline Syst. Eng. Pract.* **2021**, *12*, 04021057. [CrossRef]
- Gu, F.; Zhou, J.; Hai, H.; Song, Y. Pullout test study on flexible joint of ductile iron buried pipelines. *Adv. Mater. Res.* **2012**, *368–373*, 1130–1133. [CrossRef]
- Jang, Y.C.; Kim, I.J.; Kim, C.M.; Jeon, B.G.; Chang, S.J.; Kim, Y.P. A Study on the Deformation Characteristics of Gas Pipeline under Internal Pressure and In-Plane Bending Load. *Trans. Korean Soc. Press. Vessel. Pip.* **2019**, *15*, 50–57.

15. Varelis, G.E.; Ferino, J.; Karamanos, S.A.; Lucci, A.; Demofonti, G. Experimental and Numerical Investigation of Pressurized Pipe Elbows under Strong Cyclic Loading Conditions. In Proceedings of the ASME 2013 Pressure Vessels & Piping Division Conference, Paris, France, 14–18 July 2013.
16. Jeon, B.G.; Kim, S.W.; Choi, H.S.; Park, D.U.; Kim, N.S. A Failure Estimation Method of Steel Pipe Elbows under In-plane Cyclic Loading. *Nucl. Eng. Technol.* **2017**, *49*, 245–253. [[CrossRef](#)]
17. Kim, S.W.; Choi, H.S.; Jeon, B.G.; Hahm, D.G. Low-cycle fatigue behaviors of the elbow in a nuclear power plant piping system using the moment and deformation angle. *Eng. Fail. Anal.* **2019**, *96*, 348–361. [[CrossRef](#)]
18. Pappa, P.; Varelis, G.E.; Karamanos, S.A.; Gresnigt, A.M. Low Cycle Fatigue Tests and Simulations on Steel Elbows. In Proceedings of the ASME 2013 Pressure Vessels & Piping Division Conference, Paris, France, 14–18 July 2013.
19. Takahashi, K.; Watanabe, S.; Ando, K.; Urabe, Y.; Hidaka, A.; Hisatsune, M.; Miyazaki, K. Low cycle fatigue behaviors of elbow pipe with local wall thinning. *Nucl. Eng. Des.* **2009**, *239*, 2719–2727. [[CrossRef](#)]
20. Kim, S.W.; Chang, S.J.; Park, D.U.; Jeon, B.G. Failure criteria of a carbon steel pipe elbow for low-cycle fatigue using the damage index. *Thin-Walled Struct.* **2020**, *153*, 106800. [[CrossRef](#)]
21. Kim, S.W.; Jeon, B.G.; Hahm, D.G.; Kim, M.K. Ratcheting fatigue failure of a carbon steel pipe tee in a nuclear power plant using the deformation angle. *Eng. Fail. Anal.* **2020**, *114*, 104595. [[CrossRef](#)]
22. Nuclear Energy Agency (NEA); Committee on the Safety of Nuclear Installations (CSNI). *Integrity of Structures, Systems and Components under Design and Beyond Design Loads in Nuclear Power Plants, Final Report of the Project on Metallic Component Margins under High Seismic Loads (MECOS)*; NEA: Paris, France, 2018.
23. Soroushian, S.; Zaghi, A.E.; Maragakis, E.M.; Echevarria, A.; Tian, Y.; Filiatrault, A. Seismic fragility study of fire sprinkler piping systems with grooved fit joints. *J. Struct. Eng.* **2015**, *141*, 04014157. [[CrossRef](#)]
24. Kim, S.W.; Yun, D.W.; Jeon, B.G.; Kim, J.B. Seismic performance evaluation of a vertical pipe connected with rigid groove joints using a system and a component. *Structures* **2022**, *36*, 691–702. [[CrossRef](#)]
25. Ju, B.S.; Jeon, B.G.; Kim, S.W.; Son, H.Y. Validation of Seismic Performance of Stainless Press-to-Connect Piping System under Cyclic Loadings. *Appl. Sci.* **2022**, *12*, 3896. [[CrossRef](#)]
26. Perrone, D.; Brunesi, E.; Filiatrault, A.; Peloso, S.; Nascimbene, R.; Beiter, C.; Piccinin, R. Seismic Numerical Modelling of Suspended Piping Trapeze Restraint Installations based on Component Testing. *Bull. Earthq. Eng.* **2020**, *18*, 3247–3283. [[CrossRef](#)]
27. Kim, S.W.; Jeon, B.G.; Hahm, D.G.; Kim, M.K. Seismic fragility evaluation of the base-isolated nuclear power plant piping system using the failure criterion based on stress-strain. *Nucl. Eng. Technol.* **2019**, *51*, 561–572. [[CrossRef](#)]
28. Jeon, B.G.; Kim, S.W.; Yun, D.W.; Hahm, D.G.; Eem, S.H. Seismic Fragility Evaluation of Main Steam Piping of Isolated APR1400 NPP Considering the Actual Failure Mode. *Sustainability* **2022**, *14*, 8315. [[CrossRef](#)]
29. National Fire Protection Association (NFPA). *Standard for the Installation of Sprinkler Systems*; NFPA: Quincy, MA, USA, 2013.
30. Lv, Y.; Liu, C.F.; Huang, X.; Chen, Y.; Chou, N. Experimental and finite-element study of buried pipes connected by bellow joint under axial cyclic loading. *J. Pipeline Syst. Eng. Pract.* **2021**, *12*, 04020069. [[CrossRef](#)]
31. Kim, P.S.; Kim, J.D. Performance evaluation of the forming methods used in the production of bellows for LNG carriers I—Comparison of design methods and mechanical properties of bellows. *J. Adv. Mar. Eng. Technol.* **2016**, *40*, 587–592. [[CrossRef](#)]
32. *KS D 3631*; Carbon Steel Pipes for Fuel Gas Piping. Korea Agency for Technology and Standards (KS): Eumseong, Korea, 2020.
33. *KS D 3503*; Rolled Steels for General Structure. Korea Agency for Technology and Standards (KS): Eumseong, Korea, 2018.
34. *KGS FU551*; Facility/Technical/Inspection Code for Urban Gas Using Facilities. Korea Gas Safety Corporation (KGS): Eumseong, Korea, 2021.
35. *ANSI/FM Approvals 1950*; American National Standard for Seismic Sway Braces for Pipe, Tubing and Conduit. American National Standards Institute (ANSI): Washington, DC, USA, 2016.
36. *KS B 1528*; Seismic Safety Test Method for Pipe Connecting Parts. Korea Agency for Technology and Standards (KS): Eumseong, Korea, 2019.
37. Malhotra, P.K.; Sensory, P.E.; Braga, A.C.; Allard, R.L. Testing sprinkler-pipe seismic-brace components. *Earthq. Spectra* **2003**, *19*, 87–109. [[CrossRef](#)]
38. *FEMA 461*; Interim Testing Protocols for Determining the Seismic Performance Characteristics of Structural and Nonstructural Components. Federal Emergency Management Agency (FEMA): Washington, DC, USA, 2007.
39. *ISO 16134*; Earthquake-Resistant and Subsidence-Resistant Design of Ductile Iron Pipelines. International Organization for Standardization (ISO): Geneva, Switzerland, 2020.